Contents lists available at ScienceDirect

J Materiomics

Enhanced thermoelectric properties of SnSe thin films grown by pulsed laser glancing-angle deposition

CrossMark

Chun Hung Suen [a,1], Dongliang Shi [b,1], Y. Su [c,1], Zhi Zhang [a], Cheuk Ho Chan [a], Xiaodan Tang [d], Y. Li [c], Kwok Ho Lam [b,***], Xinxin Chen [a], B.L. Huang [c,**], X.Y. Zhou [d], Ji-Yan Dai [a,*]

[a] Department of Applied Physics, The Hong Kong Polytechnic University, Hung Hom, Kowloon, Hong Kong, China
[b] Department of Electrical Engineering, The Hong Kong Polytechnic University, Hung Hom, Kowloon, Hong Kong, China
[c] Department of Mechanical and Aerospace Engineering, The Hong Kong University of Science and Technology, Clear Water Bay, Kowloon, Hong Kong, China
[d] College of Physics, Chongqing University, Chongqing 401331, China

ARTICLE INFO

ABSTRACT

SnSe single crystals have been demonstrated to possess excellent thermoelectric properties. In this work, we demonstrate a grain size control method in growing nanocrystalline SnSe thin films through a glancing angle pulsed-laser deposition approach. Structural characterization reveals that the SnSe film deposited at a normal angle has a preferred orientation along a axis, while by contrast, the SnSe film deposited at an 80° glancing angle develops a nanopillar structure with the growth direction towards the incident atomic flux. The glancing angle deposition greatly reduces the grain size of the thin film due to a shadowing effect to the adatoms, resulting in significantly increased power factor for more than 100%. The maximum Seebeck coefficient and power factor are 498.5 $\mu V/K$ and 18.5 $\mu Wcm^{-1}K^{-2}$, respectively. The enhancement of thermoelectric property can be attributed to the potential barrier scattering at grain boundaries owing to the reduced grain size and increased grain boundaries in the film. Given this enhanced power factor, and considering the fact that the nanopillar structure should have much lower thermal conductivity than a plain film, the zT value of such made SnSe film could be significantly larger than the corresponding single crystal film, making it a good candidate for thin film-based thermoelectric device.

1. Introduction

Recent progress of thermoelectric (TE) materials study is attracting the increasing number of researchers to devote their effort to explore high-efficiency materials with higher figure of merit, zT, approaching large scale energy harvesting applications. In the meantime, the interest in TE thin film study is also increasing, especially when the low-dimensional materials (such as 2D materials) are being extensively studied worldwide. Besides the profound physics behind the TE thin film study, such as quantum confinement effect [1] and phonon dragging effect [2], etc., the main driving force for the TE thin film study is the potential application in integrated cooling devices and electronic devices such as IC chips, where the hot spot issue should be addressed through local cooling [3]. The TE thin films are also robust for supplying electrical energy to micro- and nano-devices where a thermal gradient exists. However, compared to those being extensively studied bulk TE materials, thin film-based TE materials and devices are relatively less studied. Nevertheless, there are still many materials that have been made into thin film form, such as Bi_2Te_3, Bi_2Se_3, Pb_2Te_3 [4–9] and traditional semiconductors SiGe [10].

Recently, there are some state-of-the-art TE materials such as Cu_2Se and SnSe [11–13], among those materials, SnSe shows superior TE properties including ultralow thermal conductivity. At room temperature, SnSe is a layered orthorhombic structure, with space group Pnma (a = 1.149 nm, b = 0.444 nm, c = 0.4135 nm)

* Corresponding author.
** Corresponding author.
*** Corresponding author.
E-mail address: jiyan.dai@polyu.edu.hk (J.-Y. Dai).
Peer review under responsibility of The Chinese Ceramic Society.
[1] Equal contributor.

[11,14]. Along the *b-c* plane, there are SnSe double layers with strong zigzag Sn-Se bond; while in direction along *a-*, the double layers are linked by weak van der Waals force. There are a few research studies based on the thin film form of SnSe, however, most of them are mainly for transport and optical properties that are related to an optoelectronic field [15—20]. This motivates us to study the growth and TE properties of SnSe thin film, and investigate the enhancement of those properties by controlling the grain size.

In order to enhance the TE performance, there are several approaches such as quantum confinement effect [1], band structure modification [21] and heavy band convergence [22,23] to enhance the Seebeck coefficient. *zT* is a dimensionless figure of merit governing the TE performance, and $zT = \sigma S^2 T/(\kappa_L + \kappa_e)$, where σ, S, T, κ_L and κ_e are electrical conductivity, Seebeck coefficient, absolute temperature, lattice thermal conductivity and carrier thermal conductivity respectively. *zT* consist of two parts, the first part is an electronic part called power factor, in which power factor = σS^2; while the second part is a thermal part ($\kappa_L + \kappa_e$). *zT* can also be improved by reducing the thermal conductivity, with aid of all-scale hierarchical architecture [24] and nanostructure [25]. Besides those approaches, the TE performance can also be improved by introducing grain boundaries; the influence of grain size on Seebeck coefficient, thermal conductivity and electrical conductivity has been investigated by different researchers at bulk scale [26,27] and thin film scale [28,29].

Glancing angle deposition of thin films has been demonstrated to be able to control the grain size of the films [30—32]. In glancing angle deposition, a substrate surface is nearly perpendicular to the target. During the deposition, the small angle of adatoms to the substrate causes a large shadowing effect between nuclei and prevents grains from merging, so that a film structure of nanopillar array inclined towards the target could be formed. In this work, we demonstrate the enhancement of TE performance of SnSe thin films through an approach of grain size control by the glancing angle pulsed-laser deposition method.

2. Experimental

In growing the SnSe thin film, pulsed laser deposition (PLD) was used, because it is designed for growing the chalcogenide film [33—35]. Moreover, the source flux in PLD is directional to the substrate, which is favorable for growing the nanopillar structure in glancing angle deposition. Laser source used in the experiment was KrF excimer laser, with a wavelength of 248 nm and a repetition rate of 10 Hz. The deposition time of film grown at normal angle was 30 min, while that of film grown at 80° glancing angle was doubled because of the slower glancing angle film deposition rate. The base pressure in the experiment was around 10^{-5} Torr. The target for SnSe growth was stoichiometric SnSe polycrystal. Silicon (100) was selected as the substrate, which had a top layer of 300 nm-thick amorphous SiO_2 that acted as an insulating layer between the grown SnSe film and the silicon substrate, so as to reduce the influence of the substrate to the TE performance of the film. To investigate the optimal deposition temperature of SnSe film in PLD, the substrate temperature (T_s) was varied from 250 °C to 350 °C. After the optimized deposition temperature was confirmed by transmission electron microscope (TEM) (JEOL 2100 F, operated at 200 kV) and X-ray diffraction (XRD) (Rigaku SmartLab), samples were grown based on the optimized deposition temperature, using a normal angle deposition or an 80° glancing angle deposition.

Crystalline phase and orientation of the thin film were determined by XRD, with Cu Kα_1 source. The microstructure of the thin film was determined by TEM and the composition was confirmed by energy dispersive spectroscopy (EDS) in TEM. The thickness of

the film was determined by atomic force microscope (AFM) (Asylum MFP 3D Infinity). The morphology of the as-grown film was obtained by cross-sectional scanning electron microscopy (SEM) (JEOL 6330 F) and AFM. Seebeck coefficient and electrical conductivity at a temperature range from 300 to 575 K were obtained by NETZSCH SBA 458 Nemesis. Thermal conductivity in the out-of-plane direction from 200 to 340 K was obtained by the well-accepted 3ω method [36].

3. Results and discussion

Fig. 1 shows the XRD patterns of the SnSe films deposited at 250, 310, 330 and 350 °C, respectively. Among all these samples, the peaks at 2θ = 15.4°, 31.1° and 64.8° correspond to the (200), (400) and (800) diffraction peaks of orthorhombic SnSe (a = 1.149 nm, b = 0.4153 nm, c = 0.444 nm, JCPDS #48—1224), respectively. This implies that the SnSe films are preferentially grown along *a*-axis, which is consistent with the layered structure characteristic of SnSe along *a*-axis.

Detailed XRD pattern investigations show that there are (200), (400) and (800) planes for the SnSe films deposited at 250 °C, 310 °C, 330 °C and 350 °C, while the (200) and (800) diffraction peaks significantly decrease when the deposition temperature reached 350 °C. Other than those preferential peaks mentioned, there are additional peaks (302) and (122) planes present in the SnSe film grown at low temperature of 250 °C. It is apparent that these peaks decrease when the deposition temperature reached 310 °C, and when the deposition temperature reached 350 °C, the (302) and (122) planes vanish. One can also see that some additional peaks (201), (311) and (511) planes present at higher deposition temperature (330 °C and 350 °C). Based on these detailed XRD results, it can be concluded that 330 °C is close to the optimized deposition temperature of SnSe thin film.

To understand the microstructure and chemical composition of the as-grown thin film, TEM investigations and EDS analysis were performed. Fig. 2a shows a typical high-resolution TEM image (HRTEM) of the SnSe thin film deposited at 330 °C. The detailed analysis on the lattice plane distances and angles between those lattice planes indicates that the film is orthorhombic SnSe (a = 1.149 nm, b = 0.4153 nm, c = 0.444 nm), which is consistent with the XRD result mentioned above. The EDS pattern shown in Fig. 2b indicates that the film is composed of Sn and Se (noted that the Cu peak belongs to the copper grid), and the quantitative EDS analysis shows that the ratio of composition of Sn and Se is around 1:1, suggesting the formation of SnSe compound.
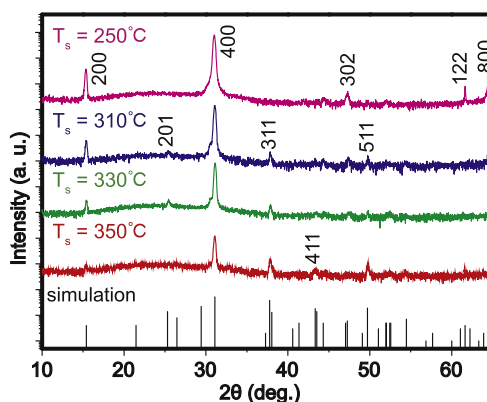

Fig. 1. XRD patterns of the SnSe thin film deposited at a normal angle and the substrate temperatures of T_s = 250 °C, 310 °C, 330 °C, 350 °C. The patterns are compared to the SnSe simulation pattern (JCPDS #48—1224).

To study the effect of glancing angle deposition on the morphology and the grain size, the other SnSe thin film was deposited at 330 °C at an 80° glancing angle. Its XRD pattern is shown in Fig. 3. The indexing of the diffraction peaks in the XRD pattern indicates that, compared to the thin film grown at a normal angle, (200) and (800) orientation do not present in the thin film grown with a glancing angle, suggesting that the growth direction and orientation is not preferential. In addition, there are many different grain orientations in the film, besides the (201) plane at $2\theta = 25.45°$ and (311) peak at $2\theta = 37.86°$ which are also present in the film deposited at a normal angle, the sample deposited with a glancing angle has also (111) diffraction, locates at $2\theta = 30.5°$, (511) plane at $2\theta = 49.73°$, (610) peak located at $2\theta = 52.47°$ and (420) orientation at a diffraction angle of $2\theta = 54.21°$. Those orientations indicate that the sample was not grown along a axis. The patterns of the two samples deposited with the normal and glancing angles are different because of their distinct morphologies and growth orientations. The film grown with glancing angle exhibits a nanopillar structure, and since the diffraction at the tip of pillar is different from that on a plain film, the XRD patterns would be different. Nevertheless, it should be noticed that the glancing angle deposited film possesses the same crystal structure as the normal angle deposited film, even their microstructures are different.

To observe the thickness and surface morphology of the SnSe thin films grown with the normal and glancing angles, AFM and SEM were performed to obtain their top view images. By measuring the height difference between the bear substrate and the thin film, the thickness of SnSe thin film is 730 nm for the sample grown with the normal angle deposition for 30 min, while it is 300 nm for the sample grown with the glancing angle deposition for 60 min. Fig. 4a and b shows the morphology of thin films deposited at the normal and glancing angles respectively, and they can be compared with the SEM top view images as shown in Fig. 4c and d. It can be observed that the film deposited at a normal angle (Fig. 4a and c) shows some local maximum points while there are large grains locate between those maximum points. In contrast, for the sample grown at a glancing angle, the top view images in Fig. 4b and d shows that a nanopillar structure rather than a continuous film on the substrate. These nanopillars incline towards a specific direction, suggesting that the pillars grow towards the direction of the incident flux [30,31]. In addition, the nanopillars are grown with a relatively high density. In terms of grain size, the SnSe film deposited at a normal angle has an average grain size of ~730 nm with the root-mean-square surface roughness (R_q) of the film of 17 nm, while that deposited at a glancing angle has a grain size of ~120 nm with the R_q of 54 nm. These results indicate that the grain size of film grown at a normal angle is about six times larger than that of sample deposited at a glancing angle. Meanwhile, the film
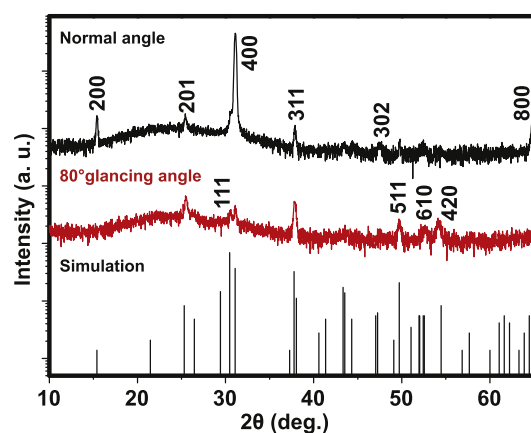

Fig. 3. XRD patterns of the thin film deposited at a normal angle and an 80° glancing angle with $T_s = 330$ °C. The patterns are compared to the SnSe simulation pattern (JCPDS #48−1224).

grown at normal angle is much smooth than that grown at glancing angle.

Cross-sectional SEM investigations were also performed to further understand the morphology of the film. Fig. 4e and f shows the SEM images of the two samples grown at the normal and glancing angles, respectively. As shown in Fig. 4e, the sample deposited at a normal angle shows a continuous columnar structure pointing upward. In contrast, the sample deposited at a glancing angle shows many slanted nanopillars on the substrate surface, which is well consistent with the AFM results. These detailed studies indicate that the samples grown at a normal angle and a glancing angle have totally different morphologies and crystal orientations.

TE measurements were performed on the samples deposited at the normal and glancing angles, and the results are shown in Fig. 5, including Seebeck coefficient (Fig. 5a), electrical conductivity (Fig. 5b), power factor (Fig. 5c) and out-of-plane thermal conductivity (Fig. 5d). In terms of Seebeck coefficient, both films show the positive Seebeck coefficients, indicating that the SnSe thin films are the p-type material. In addition, the temperature dependence of Seebeck coefficient on the two samples is similar within the temperature range of 300−578 K, which can be described in two regions. In the first region, the Seebeck coefficient increases with the temperature from room temperature and reaches their maximum at 477 and 426 K for the films deposited at the normal and glancing angles, respectively. Specifically, the maximum Seebeck coefficient of the film deposited at a normal angle is about 193.7 $\mu V/K$ at 477 K, while the maximum Seebeck coefficient of the film
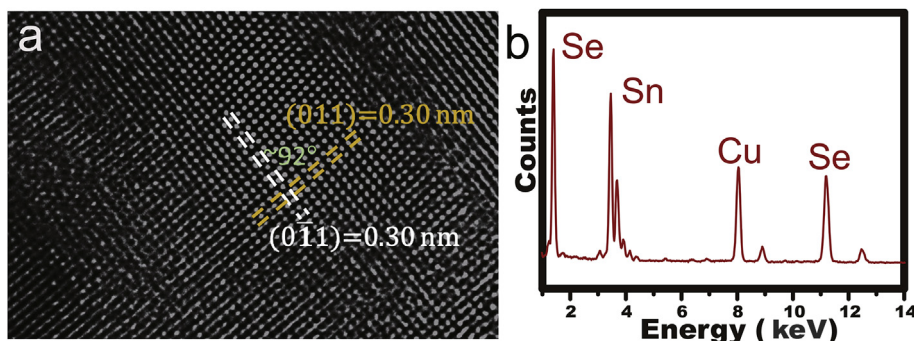

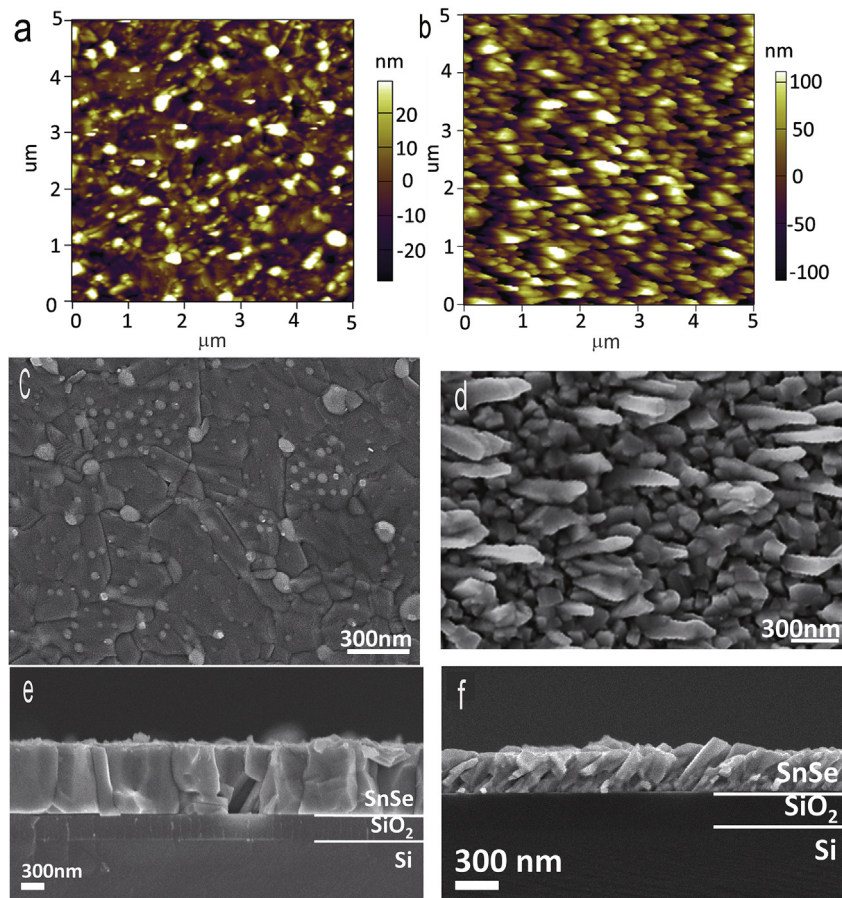Fig. 2. (a) HRTEM image and (b) EDS spectrum of SnSe thin film deposited at a normal angle with $T_s = 330$ °C.

Fig. 4. AFM images of SnSe thin films deposited at (a) normal angle and (b) glancing angle and T_s = 330 °C. Top view SEM images of films deposited at (c) normal angle and (d) glancing angle and T_s = 330 °C. Cross sectional SEM images of films grown at (e) normal angle and (f) glancing angle and T_s = 330 °C.

deposited at a glancing angle is much higher, 498.5 $\mu V/K$ at 426 K. After reaching the peak, the Seebeck coefficients of the two films decrease, and converge in the second region in which the co-efficients reach negative at the highest measured temperature of ~579 K. According to previous study [27], this phenomenon is due to the increasing intrinsic electron carrier concentration by thermal excitation.

For the temperature dependence of electrical conductivity, both samples show the semiconducting characteristic. From 300 to 426 K, the electrical conductivities of the samples increase steadily, after 426 K, both samples are thermally activated such that the conductivities increase exponentially, which is consistent to the drop of Seebeck coefficient. Both films show the same trend without a significant difference in terms of electrical conductivity.

As shown in Fig. 5c, the power factor of SnSe film deposited at a glancing angle shows the highest value of 18.5 $\mu W cm^{-1} K^{-2}$ at 478 K. Compared to the film grown at normal angle, the power factor of the film deposited at glancing angle is enhanced signifi-cantly (>20 times higher). The enhancement of power factor is mainly contributed by the increase of Seebeck coefficient. The increment of Seebeck coefficient via the grain size control strategy can be explained by potential barrier scattering at grain boundaries. This concept has been investigated in theoretical and experimental ways, for bulk and thin film scales [26,27,29]. Given a TE material with one type of mobile carrier, after a constant thermal gradient is applied onto the material, the carriers in the material will move from the hot side to the cold side by diffusion so as to induce the Seebeck voltage. Consequently, a potential difference will be

developed on the both sides, drifting the mobile charge carrier back to the original position and diminishing the Seebeck voltage.

In the whole procedure, the diffusion produces the Seebeck voltage and the drift subtracts it. Therefore, if there is a potential barrier to retard or even stop the drift of carriers, the Seebeck co-efficient can be enhanced. Here in this study, the grain boundary is the potential barrier to filter and scatter the carriers, such that the carriers with lower energy compared to the barrier are stopped, while the carriers with higher energy can pass through the barrier. The SnSe thin film grown with the glancing angle increases the surface area of grain boundary and scatters the carriers much effectively. Moreover, similar to the previous study [26], the effect of grain size on the Seebeck coefficient is temperature dependence. In Fig. 5a, the two samples have a relatively large Seebeck coeffi-cient difference at low temperatures, but the difference becomes very small as their Seebeck coefficients converge at high temper-atures beyond 426 K. This is because the carriers do not have enough energy to overcome the potential barrier at low tempera-tures, so the large number of grain boundaries existed in the film deposited with the glancing angle can scatter the carriers effi-ciently, resulting in a large increase of Seebeck coefficient. At high temperatures, the drift cannot be stopped as the carriers have enough kinetic energy to pass through the grain boundaries, resulting in the inefficient enhancement of Seebeck coefficient even for the film deposited at a glancing angle. Therefore, the Seebeck coefficients of the two films converge eventually at high temperatures.

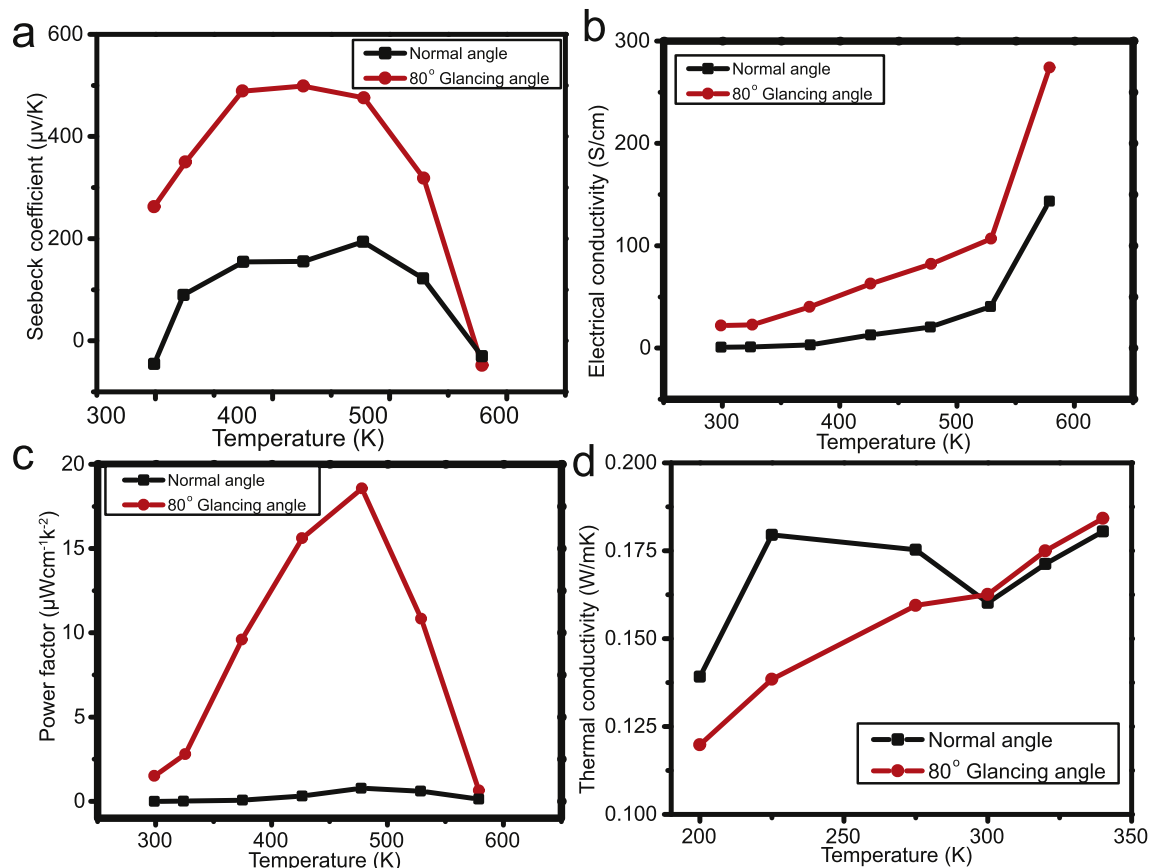The out-of-plane thermal conductivities of the two films have

Fig. 5. TE properties of SnSe thin films as a function of temperature. (a) Seebeck coefficient. (b) Electrical conductivity. (c) Power factor and (d) Thermal conductivity.

been measured with a temperature range from 200 to 340 K. In Fig. 5d, from 200 to 300 K, the film deposited at a normal angle has higher thermal conductivity, while beyond 300 K, the conductivities of the two as-deposited films do not have significant difference. The overall temperature dependence of thermal conductivities of films is increasing with the temperature, and they reach the highest value of ~0.189 W/mK at 340 K. The temperature dependence of thermal conductivity may be due to the lower dimension of thin film, contribution of phonon to thermal conductivity is confined, and charge carriers dominate the conduction of heat. Therefore, similar with the trend of electrical conductivity, thermal conductivity increases with temperature.

When compared the TE performance of SnSe thin film sample deposited at a glancing angle with its bulk single crystal counterpart [11], the film in the present study has a lower operation temperature than the bulk material. For the bulk material, the SnSe single crystal has the highest power factor of 10.1 $\mu Wcm^{-1}K^{-2}$ at ~973 K. The lower operation temperature of the thin film compared to the bulk single crystal may be due to the reduction of material dimension. Compared to the SnSe thin films deposited by other researchers [16], the room temperature Seebeck coefficient of the sample in the present study (262.2 $\mu V/K$) is lower, while the room-temperature Seebeck coefficients in previous study on different substrates were from 432 $\mu V/K$ to 505 $\mu V/K$. Compared to the bulk single crystal SnSe [11], the increasing trend of out-of-plane thin film thermal conductivity is different from that of bulk SnSe, which has a decreasing trend. The films in this study have much lower thermal conductivities, and we believe that the difference should be due to the grain and surface boundary scattering. Since the out-of-plane thermal conductivity cannot be used directly with in-

plane electrical properties to evaluate zT, we will not give a particular value of zT in this paper, even based on a very conservative estimation the zT value could be much higher than the bulk single crystal. We will report the in-plane thermal conductivity and zT value elsewhere.

4. Conclusion

Polycrystalline SnSe thin films were prepared by using PLD at a normal and an 80° glancing angle on silicon substrates with a 300 nm-thick of silicon oxide. The results reveal that the glancing angle deposition can greatly reduce the grain size of the thin film and significantly enhance the Seebeck coefficient and power factor. The enhancement thermoelectric property can be attributed to the potential barrier scattering at grain boundaries owing to the reduced grain size and increased grain boundaries in the film. This study provides an alternative strategy to enhance the thermoelectric performance of thin films.

References

[1] Hicks LD, Dresselhaus MS. Effect of quantum-well structures on the thermoelectric figure of merit. Phys Rev B 1993;47(19):12727–31.
[2] Wang G, Endicott L, Chi H, Lost'ak P, Uher C. Tuning the temperature domain of phonon drag in thin films by the choice of substrate. Phys Rev Lett 2013;111:046803.

[3] Lin S-C, Banerjee K. Cool chips: opportunities and implications for power and thermal management. IEEE Trans Electron Dev 2008;55(1):245–55.

[4] Lin J-M, Chen T-C, Lin C-P. Annealing effect on the thermoelectric properties of Bi$_2$Te$_3$ thin films prepared by thermal evaporation method. J Nanomater 2013;2013:1–6.

[5] Goldsmid HJ. Bismuth telluride and its alloys as materials for thermoelectric generation. Materials 2014;7:2577–92.

[6] Touzelbaev MN, Zhou P, Venkatasubramanian R, Goodson KE. Thermal characterization of Bi$_2$Te$_3$/Sb$_2$Te$_3$ superlattices. J Appl Phys 2001;90:763–7.

[7] Beyer H, Nurnus J, Bottner H, Lambrecht A, Wagner E, Bauer G. High thermoelectric figure of merit ZT in PbTe and Bi2Te3-based superlattices by a reduction of the thermal conductivity. Phys E 2002;13:965–8.

[8] Zeipl R, Jelínek M, Kocourek T, Remsa J, Vlcek JVM. Properties of thermoelectric nanocomposite Bi$_2$Te$_3$ layers prepared by PLD. Sensors Transducers 2014;183:103–9.

[9] Collins-McIntyre LJ, Wang W, Zhou B, Speller SC, Chen YL, Hesjedal T. Growth of Bi$_2$Se$_3$ and Bi$_2$Te$_3$ on amorphous fused silica by MBE. Phys Status Solidi B 2015;252(6):1334–8.

[10] Joshi G, Lee H, Lan Y, Wang X, Zhu G, Wang D, et al. Enhanced thermoelectric figure-of-merit in nanostructured p-type silicon germanium bulk alloys. Nano Lett 2008;8(12):4670–4.

[11] Zhao L-D, Lo S-H, Zhang Y, Sun H, Tan G, Uher C, et al. Ultralow thermal conductivity and high thermoelectric figure of merit in SnSe crystals. Nature 2014;508(7496):373–7.

[12] Peng K, Lu X, Zhan H, Hui S, Tang X, Wang G, et al. Broad temperature plateau for high ZTs in heavily doped p-type SnSe single crystals. Energy Environ Sci 2016;9(2):454–60.

[13] Liu H, Shi X, Xu F, Zhang L, Zhang W, Chen L, et al. Copper ion liquid-like thermoelectrics. Nat Mater 2012;11(5):422–5.

[14] Li CW, Hong J, May AF, Bansal D, Shi S, Hong T, et al. Orbitally driven giant phonon anharmonicity in SnSe. Nat Phys 2015;11(12):1063–9.

[15] Urmila KS, Namitha TA, Rajani J, Philip RR, Pradeep B. Optoelectronic properties and seebeck coefficient in SnSe thin films. J Semicond 2016;37:093002.

[16] Inoue T, Hiramatsu H, Hosono H, Kamiya T. Heteroepitaxial growth of SnSe films by pulsed laser deposition using Se-rich targets. J Appl Phys 2015;118(20):205302.

[17] Indirajith R, Rajalakshimi M, Gopalakrishnan R, Ramamurthi K. Effects of annealing on thermally evaporated SnSe thin films. Ferroelectrics 2011;413(1):108–14.

[18] John KJ, Pradeep B, Mathai E. Tin selenide (SnSe) thin films prepared by reactive evaporation. J Mater Sci 1994;29:1581–3.

[19] Quan DT. Electrical porperties and optical absorption of SnSe evaporated thin films. Phys Status Solidi A 1984;86:421–6.

[20] Rao TS, Chaudhuri AK. Electrical and photoelectronic properties of SnSe thin films. J Phys D Appl Phys 1985;18. L35–L9.

[21] Heremans JP, Jovovic V, Toberer ES, Saramat A, Kurosaki K, Charoenpha A. Enhancement of thermoelectric efficiency in PbTe by distortion of the electronic density of states. Science 2008;321:554–7.

[22] Pei Y, Shi X, LaLonde A, Wang H, Chen L, Snyder GJ. Convergence of electronic bands for high performance bulk thermoelectrics. Nature 2011;473(7345):66–9.

[23] Liu W, Tan X, Yin K, Liu H, Tang X, Shi J, et al. Convergence of conduction bands as a means of enhancing thermoelectric performance of n-type Mg$_2$Si$_{1-x}$Sn$_x$ solid solutions. Phys Rev Lett 2012;108(16):166601.

[24] Biswas K, He J, Blum ID, Wu C-I, Hogan T-P, Seidman DN, et al. High-Performance bulk thermoelectrics with all-scale hierarchical architectures. Nature 2012;489:414–8.

[25] Hsu KF, Loo S, Guo F, Chen W, Dyck JS, Uher C, et al. Cubic AgPb$_m$SbTe$_{2+m}$: bulk thermoelectric materials with high figure of merit. Science 2004;303:818–21.

[26] Gao Y, He Y, Zhu L. Impact of grain size on the Seebeck coefficient of bulk polycrystalline thermoelectric materials. Chin Sci Bull 2010;55(1):16–21.

[27] Kuo C-H, Chien H-S, Hwang C-S, Chou Y-W, Jeng M-S, Yoshimura M. Thermoelectric properties of fine-grained PbTe bulk materials fabricated by cry-omilling and spark plasma sintering. Mater Trans 2011;52(4):795–801.

[28] Takashiri M, Miyazaki K, Tanaka S, Kurosaki J, Nagai D. Effect of grain size on thermoelectric properties of n-type nanocrystalline bismuth-telluride based thin films. J Appl Phys 2008;104(8):084302.

[29] Valalaki K, Vouroutzis N, Nassiopoulou AG. Significant enhancement of the thermoelectric figure of merit of polycrystalline Si films by reducing grain size. J Phys D Appl Phys 2016;49(31):315104.

[30] Robbie K, Brett MJ. Sculptured thin films and glancing angle deposition: growth mechanics and applications. J Vac Sci Technol A Vac Surfaces Films 1997;15(3):1460–5.

[31] Zhao Y-P, Ye D-X, Wang G-C, Lu T-M. Designing nanosturctures by glancing angle deposition. Proc SPIE 2003;5219:59–71.

[32] Wang H-h, Zhao Y-P. Nanostructure evolution of YBa$_2$Cu$_3$O$_x$ thin films grown by pulsed-laser glancing-angle deposition. J Vac Sci Technol B Microelectron Nanom Struct 2006;24(3):1230–3.

[33] Hiramatsu H, Ohta H, Hirano M, Hosono H. Heteroepitaxial growth of single-phase zinc blende ZnS films on transparent substrates by pulsed laser deposition under H$_2$S atmosphere. Solid State Commun 2002;124:411–5.

[34] Hiramatsu H, Ohta H, Suzuki T, Honjo C, Ikuhara Y, Ueda K, et al. Mechanism for heteroepitaxial growth of transparent P-Type semiconductor: LaCuOS by reactive solid-phase epitaxy. Cryst Growth Des 2004;4.

[35] Hiramatsu H, Kamioke H, Ueda K, Ohta H, Kamiya T, Hirano M, et al. Optoelectronic properties and light-emitting device application of widegap layered oxychalcogenides: LaCuOCh(Ch= chalcogen) and La2CdO2Se2. Phys Status Solidi A 2006;203(11):2800–11.

[36] Cahill DG. Thermal conductivity measurement from 30 to 750 K: the 3ω method. Rev Sci Instrum 1990;61:802–8.

Chun Hung Suen is an M.Phil. Student in The Hong Kong Polytechnic University. He received his Bachelor of Science degree in Engineering Physics [Optoelectroics] from The Hong Kong Polytechnic University, in 2015. He started his Master's Degree as a member of Ji-Yan Dai's group in 2015. He is mainly focus on exploiting thermoelectric thin films currently.

Dai Jiyan is currently a Professor of the Department of Applied Physics at The Hong Kong Polytechnic University. Prof. Dai's main research interests include nanomaterials fabrication and application, especially functional oxide thin films and devices. He received his B·Sc. degree in physics from Fudan University in 1988, his M.S. degree in Electronic Engineering from Tsinghua University in 1991, and his Ph.D. degree in Materials Physics from the Chinese Academy of Sciences in 1994. He has three years post-doctoral research experience at Northwestern University, and after one year working in the Institute of Materials Research and Engineering Singapore, he joined Chartered Semiconductor Manufacturing Ltd. of Singapore. Since 2001, Prof. Dai has been working at the Department of Applied Physics, The Hong Kong Polytechnic University.